1-1-2014

Recent Developments in R.F. Magnetron Sputtered Thin Films For pH Sensing Applications - An Overview

Devendra Maurya
Edith Cowan University

Ali Sardarinejad
Edith Cowan University

Kamal Alameh
Edith Cowan University

10.3390/coatings4040756
Maurya, D. , Sardarinejad, A. , & Alameh, K. (2014). Recent Developments in R.F. Magnetron Sputtered Thin Films for pH Sensing Applications - An Overview. Coatings, 4(4), 756-771. Available here

Coatings **2014**, *4*, 756-771; doi:10.3390/coatings4040756

OPEN ACCESS

coatings

ISSN 2079-6412

www.mdpi.com/journal/coatings

Review

Recent Developments in R.F. Magnetron Sputtered Thin Films for pH Sensing Applications—An Overview

D. K. Maurya *, A. Sardarinejad and K. Alameh

Electron Science Research Institute, Edith Cowan University, Joondalup, WA 6027, Australia;
E-Mails: sardarinejad@gmail.com (A.S.); k.alameh@ecu.edu.au (K.A.)

* Author to whom correspondence should be addressed; E-Mail: d.maurya@ecu.edu.au;
Tel.: +61-863-042-868; Fax: +61-863-042-908.

External Editor: Joaquim Carneiro

Received: 30 September 2014; in revised form: 21 November 2014 / Accepted: 24 November 2014 / Published: 1 December 2014

Abstract: pH sensors are widely used in chemical and biological applications. Metal oxides-based pH sensors have many attractive features including insolubility, stability, mechanical strength, electrocatalyst and manufacturing technology. Various metal oxide thin films prepared by radio frequency (R.F.) magnetron sputtering have attractive features, including high pH sensitivity, fast response, high resolution, good stability and reversibility as well as potential for measuring pH under conditions that are not favourable for the commonly used glass electrodes-based pH sensors. In addition, thin film pH sensors prepared by R.F. magnetron sputtering offer many advantages, such as ease of packaging, low cost through the use of standard microfabrication processes, miniaturisation, capability of measuring pH at high temperatures, ruggedness and disposability. In this paper, recent development of R.F. magnetron sputtered thin films for pH sensing applications are reviewed.

Keywords: R.F. magnetron sputtering; pH sensor; thin film; metal-oxides

---

1. Introduction

Nearly all processes involving water require accurate pH monitoring. Most living things rely on a proper pH level to sustain life. All human beings and animals rely on internal mechanisms to maintain

the pH level of their blood, which must be between 7.35 and 7.45. Exceeding this range could prove fatal. Additionally, dysregulated pH in human tumours has been shown to be correlated with tumour progression and malignancy [1]. Optimal soil pH provides best growth condition and high crop yields for corn, wheat and other plants as well as food products. Appropriate pH control retains milk from turning sour, prevents shampoo from hurting our eyes and makes strawberry jelly gel. The pH of wastewater leaving manufacturing plants, purification plants as well as potable water from municipal drinking water plants, must be within a specific pH range that is set forth by regulatory agencies. Other pH applications include neutralization of effluent in steel, pulp and paper, chemical, pharmaceutical manufacturing, cyanide destruction, odour scrubbers, reverse osmosis, pharmaceutical manufacturing, chemical and petrochemical manufacturing. Simply, pH is an integral part of our everyday life [2–4].

The well-known glass electrode is the most commonly used pH sensor because of desirable characteristics, such as good sensitivity, stability, and long lifetime [5,6]. However, traditional glass electrodes have many disadvantages, such as high cost, mechanical fragility, difficult to miniaturize, need for wet storage, large size and limited shape. To overcome these drawbacks and further expand the application fields, alternative pH sensor structures based on ion-sensitive field effect transistor (ISFET) [7–9], solid state [10,11], hydrogel [12,13], and microelectrode [14,15], have been reported.

Among different materials, metal oxides, in particular, offer many advantages in terms of pH sensing including insolubility, stability, mechanical strength, electrocatalyst and manufacturing technology. In recent years, a number of metal oxides based pH sensors have been developed incorporating IrO_2 [16–19], RuO_2 [20–24], PtO_2 [25], SnO_2 [25], TaO_2 [25], TiO_2 [25,26] and Ta_2O_5 [27,28]. pH sensors have been developed using a variety of deposition techniques including magnetron sputtering [20–22], sol-gel [17,29], screen-printing [24,30] and plasma enhanced chemical vapour deposition (PECVD) [31,32] and electroplating [33–35]. Among the different thin film deposition techniques, magnetron sputtering has become the process of choice for the deposition of a wide range of materials. Magnetron sputtering is extensively used in the semiconductor industry for the deposition of various materials significant for integrated circuit fabrication. Thin film sensors and photovoltaic thin films are just some of the various applications of this method. In particular, owing to its compatibility with conventional microfabrication processes, magnetron sputtering technique is advantageous in terms of high-throughput production and fabrication of high density, high quality thin films. Recently, various materials including RuO_x, RuN, SnO_2, a-WO_3, AlN, TiO_2, WO_3-IrO_2, deposited using R.F. magnetron sputtering, have demonstrated excellent capabilities for pH sensing applications.

In this paper, we review the recent developments in magnetron sputtered thin films for pH sensing applications with particular emphasis on the pH sensitivity, response time, drift rate, stability as well as potential for measuring pH under conditions that are not favourable for the commonly used glass electrodes-based pH sensors.

2. R.F. Magnetron Sputtering

In a basic sputtering process, a target (or source) material, to be deposited onto a substrate, is bombarded by energetic ions, typically inert gas ions, such as Argon (Ar^+). The forceful collision of these inert gas ions onto the target causes the removal (known as sputtering) of target atoms, which condense on the substrate as a thin film of stoichiometry similar to that of the target material. Though,

the basic idea of operation is apparently simple, the actual mechanisms involved in sputtering are quite complex. Nonetheless, the process is limited by low deposition rates, high substrate heating and low ionization efficiencies. These limitations have been overcome by the development of magnetron sputtering system.

Magnetron sputtering is now considered as the most effective process for the deposition of a wide range of thin film materials [36–40]. The main driving force behind this development has been the increasing demand for high quality functional thin films in many diverse market sectors. In many cases, magnetron sputtered films now outperform films deposited by other physical vapour deposition processes, and can offer the same functionality as much thicker films produced by other surface coating techniques. Magnetron sputtering systems generate a strong magnetic field near the target area, which causes the travelling electrons to spiral along magnetic flux lines near the target. This arrangement confines the plasma near the target area without causing the damage to the thin films being formed on the substrate, and maintains the stoichiometry and thickness uniformity of the deposited thin film. Moreover, in an R.F. magnetron sputtering systems, the generated electrons travel a longer distance, hence increasing the probability of further ionizing the inert gas atoms (Ar^+) and generating stable high-density plasma that improves the sputtering process efficiency. Figure 1 illustrates the basic components of an R.F. magnetron sputtering system. Briefly, ionised Ar atoms bombard a sputtering target, thus releasing the molecules/atoms that form thin layers on a substrate.

Figure 1. Schematic diagram illustrating the basic components of a magnetron sputtering system.

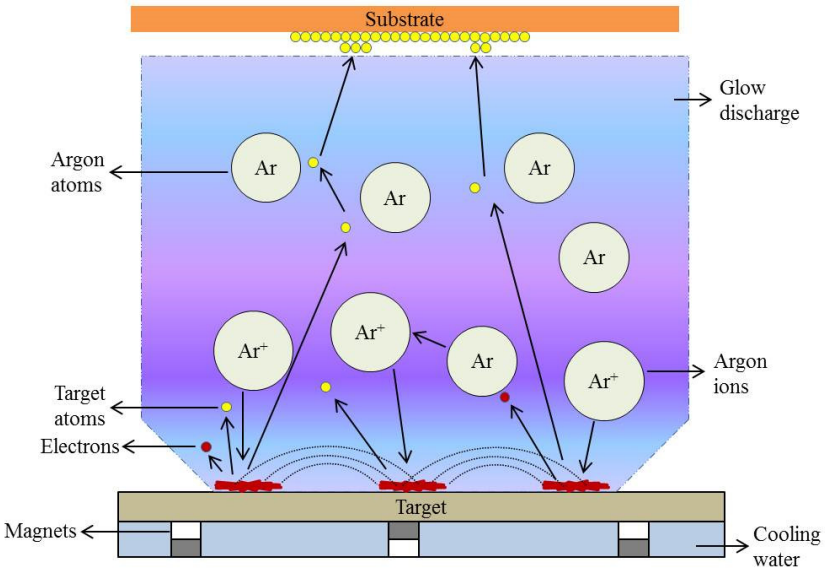

R.F. magnetron sputtering offers additional advantages, including the use of non-conductive targets, charge-up effects and reduced arching due to the use of alternating electric field (R.F. frequency). It is important to note that R.F. magnetron sputtering is especially advantageous in the deposition of thin films using non-conductive target materials. This is at the cost of R.F. power supplies and an impedance matching network between the R.F. generator and the sputtering target. It should also be noticed that without the use of a magnetron, the non-conducting materials may have more difficulty forming into a thin film as they become positively charged. Reactive sputtering can also be used, whereby the deposited film is formed by chemical reaction between the target material and the gas introduced into the vacuum

chamber. Oxides and nitrides are examples of thin films developed through reactive sputtering, where the compositions of these films can be controlled by adjusting the relative pressures of the inert and reactive gases.

3. pH Sensing Mechanism

pH measurements have conventionally relied on either optical [41–45] or electrochemical techniques [46–50]. Optical methods offer high sensitivity and non-invasiveness, however, they often require the use of dyes, which can change their optical properties due to interactions with specific analytes. In addition, quantitatively precise optical measurements are typically not straightforward due to the drift of optoelectronic components, such as light source, detector and dye concentration variations. Therefore, it is often necessary to also utilize reference dyes in optical pH measurement methods. On the other hand, electrochemical methods are typically straightforward and inherently quantitative, and require simpler operation and setups. Electrochemical methods, however, have downsides, such as long-term instability and vulnerability to electrode fouling, but nevertheless, they are the most commonly used methods for pH detection, whereby the potential (potentiometric) [20,21,51–56], current (amperometric) [57–63], or charge in an electrochemical cell serve as the analytical signals. Indeed, the glass electrode is currently the most commonly used electrochemical sensor for potentiometric pH measurements.

Potentiometry is the most preferred technique for monitoring the pH value of aqueous solutions in process control and continuous in-line measurements. In this method, the potential difference between a sensing electrode and a reference electrode immersed in the test solutions is measured. The reference electrode provides a stable constant reference potential while the ion selective electrode (sensing electrode) responds to the change of the hydrogen ion (H^+) concentration in the solution. Potentiometry-based pH sensors developed using R.F. magnetron sputtering mainly consist a metal-oxide or metal-nitride sensing electrode and a silver/silver chloride (Ag/AgCl) reference electrode. The Ag/AgCl reference electrode either consists of a silver-chloride-coated silver wire immersed in an electrolyte solution or screen-printed using Ag/AgCl paste. The equilibrium reaction governing the Ag/AgCl electrode potential response is given by [6,12]:

$$\mathrm{AgCl_{(s)} + e^- \leftrightarrow Ag_{(s)} + Cl^-_{(aq)}} \tag{1}$$

Therefore the equilibrium potential of the electrode can be expressed by the Nernstian equation:

$$E = E^0 + (RT / nF)\ln(a_{\mathrm{AgCl}}) / (a_{\mathrm{AgCl^-}}) \tag{2}$$

where E^0 is the reference electrode potential in Volt, R is the universal gas constant, T is the absolute temperature in Kelvin, n is the number of electrons involved in the reaction, F is the Faraday constant, a_x is the activity of species x (AgCl, Ag or Cl^-). The Nernstian equation for a cell is often articulated in terms of base 10 logarithms as follows:

$$E = E^0 - 0.592\log\left|\mathrm{Cl^-}\right| + 0.0592\log(k) \tag{3}$$

where *k* is the ratio of AgCl to Ag concentration. Nernstian behaviour is demonstrated by the electrode when the measured electrode potential decreases by 59 mV for every decade change in Cl^- concentration at room temperature of 25 °C.

Fog and Buck proposed five possible interpretations for the pH response mechanism of metal oxides, with the most recognized theory being oxygen intercalation [25]. The following equilibrium reaction represents the oxygen intercalation mechanism:

$$Mo_x + 2\delta H^+ + 2\delta e \leftrightarrow Mo_{x-\delta} + \delta H_2O \quad (4)$$

where MO_x is a higher metal oxide, $MO_{x-\delta}$ is a lower metal oxide and δ is the oxygen intercalation.

The Nernst's mathematical equation predicting the potential between the sensing and reference electrodes *versus* the pH value is given by [21]:

$$E = E^0 - 2.303(RT/F)\text{pH} = E^0 - 0.05916\text{pH} \quad (5)$$

The term 2.303 (*RT*/*F*) is called the Nernst slope, which is 59.16 mV/pH at room temperature (25 °C).

4. pH Sensor Performance

4.1. Sensitivity

The sensitivity of a pH electrode is determined by the linear slope response of the pH electrode as defined by the Nernst equation. It is represented in the unit of mV/pH [64].

4.2. Response Time

The response time is defined as the time at which the pH concentration in a solution is changed on contact with a pH sensor and a reference electrode has reached 95% (or 90%) of the final value. The response time is reported as $t_{95\%}$ or $t_{90\%}$ in seconds or minutes [5,64].

4.3. Drift Rate

The potential drift is defined as the difference between the peak potential value and the 90% value of the saturated potential. The potential drift measured over time is drift rate and generally represented in mV/h [64].

4.4. Hysteresis

Hysteresis is defined as the difference in the electrochemical potentials measured at same pH level. The electrochemical potentials at the same pH level may be different due to various factors, such as different oxidation states and the degree of hydration on the film surfaces, which may establish a new equilibrium of ions every time in the redox reactions at different times of testing [5,64]. In potentiometric measurements, it is represented in mV.

4.5. Temperature Coefficient of Sensitivity

The temperature coefficient of sensitivity (TCS) is an important parameter that is typically used to compensate for temperature variations, and evaluate the effect of temperature on the output voltage of the pH sensor. The TCS of the pH sensor is represented in mV/pH °C [65,66].

4.6. Reversibility

Reversibility is an essential property in pH measurements for practical applications. To evaluate the reversibility, the pH sensor potential is measured in different pH solutions in the acid-to-base direction and *vice versa* [5,21].

4.7. Resolution

The resolution of a pH sensor is defined as the minimum change in pH above the noise floor that can be detected by the pH-sensor [64,67].

5. pH Sensing Materials and Applications

Table 1 shows the summary of pH sensing materials prepared by R.F. magnetron sputtering in recent years. pH sensors are generally characterised using the buffer solutions of known pH values before applying the sensor for real time pH monitoring. Recently, we have developed pH sensor consisting R.F. magnetron sputtered ruthenium oxide (RuO_2) sensing electrode in conjunction with an on-chip integrated Ag/AgCl reference electrode. A 99.95% pure RuO_2 sputtering target was used to sputter 50 nm, 175 nm, 300 nm and 425 nm RuO_2 thin-films in 90% Ar + 10% O_2 environment with R.F. power 100 W at 1 mTorr process pressure. Potentiometric measurement has been used to test the sensor in buffer solutions of pH 4, pH 7 and pH 10. Figure 2 shows the schematic representation of potentiometric measurement setup. Briefly, in the experiments, a unity-gain amplifier was developed and used as a buffer amplifier to provide impedance matching, therefore preventing signal loss. An Agilent 34410A high performance digital multimeter was used for real-time potential recording, which has a built-in web interface that makes it easy to setup and transfer readings using only a PC with web browser. Figure 3 shows measured sensor potential *versus* pH value for different RuO_2 thin-film thicknesses [21]. Furthermore, effect of RuO_2 sensing electrode thickness on the performance of pH sensing was investigated. The thin film RuO_2 sensing electrode with thickness ranging from 50 nm to 425 nm were prepared using 99.95% pure RuO_2 sputtering target with R.F. power 100 W in 90% Ar + 10% O_2 environment at 1 mTorr process pressure. The highest sensitivity of 68.63 mV/pH was reported for RuO_2 film thickness of 300 nm when tested in buffer solutions of pH 4, pH 7 and pH 10.

Figure 4 shows the response time *versus* the RuO_2 thin-film thickness for different pH test solutions. For 50 nm thick RuO_2 film, the measured response times were 3 s, 10 s and 73.5 s for pH 4, pH 7 and pH 10, respectively. For 175 nm thick RuO_2 film, the response times for pH 4, pH 7 and pH 10 were from 3 s, 4 s and 22.5 s, respectively. On the other hand, when the thickness of the RuO_2 film was increased to 300 nm, the response times for pH 4, pH 7 and pH 10 were 3 s, 8 s and 3 s, respectively. The results in Figure 4 demonstrate that a faster response time can be attained by increasing the RuO_2 thin-film thickness up to 300 nm [21]. The pH sensor stability measured in pH 4, pH 7 and pH 10

solutions is assessed through the measured potential-versus-time curves shown in Figure 5. It is evident from Figure 5 that the sensing film thickness of 300 nm shows stable potential outputs for all pH values. The pH sensor reversibility was also investigated by switching the pH sequentially in pH loop (4-7-10-7-4). Figure 6 shows the average measured potentials for different RuO_2 thin film thicknesses. The experimental results in Figure 6 demonstrate an excellent reversibility and stable pH sensor's response for a sensing film thickness of 300 nm.

Table 1. Magnetron sputtered pH sensing materials and their performances.

pH sensing material	Sputtering target material	pH test solution	pH Sensitivity (mV/pH)	Response time (s)	Drift rate (mV/h)	Hysteresis (mV)	Ref.
RuO_2	RuO_2	4–10	58.5	< 3	–	–	[20]
RuO_2	Ru	4–10	49.8–59.1	< 1	0.38	4.36	[22]
RuN-RuO_x	Ru	1-13	55.52–57.05	30	–	–	[23]
Ta_2O_5	Ta	1–10	56.19	–	–	~5	[28]
SnO_2	SnO_2	2–12	59	–	–	7–11	[68]
TiO_2:Ru	TiO_2, Ru	1–13	55.20	< 1	1.03–1.16	–	[69]
IrO_2 & Ta_2O_5	Ir, Ta_2O_5	2–13	59.44–59.50	< 15	< 0.1	–	[70]
AlN	Al	4–10	54.5	–	–	–	[71]
TiO_2	TiO_2	1–13	56.21	–	–	–	[72]
WO_3-IrO_2	WO_3-Ir	2–12	0.168 μA/pH	< 7	–	–	[73]
RuO_x	Ru	5.5–11	52–58	< 2	1–2	–	[74]
$GdTi_xO_y$	Gd, Ti	2–12	64.13	–	0.4	< 1	[75]

Figure 2. Schematic representation of potentiometric measurement setup (S.E.—sensing electrode; R.E.—reference electrode).

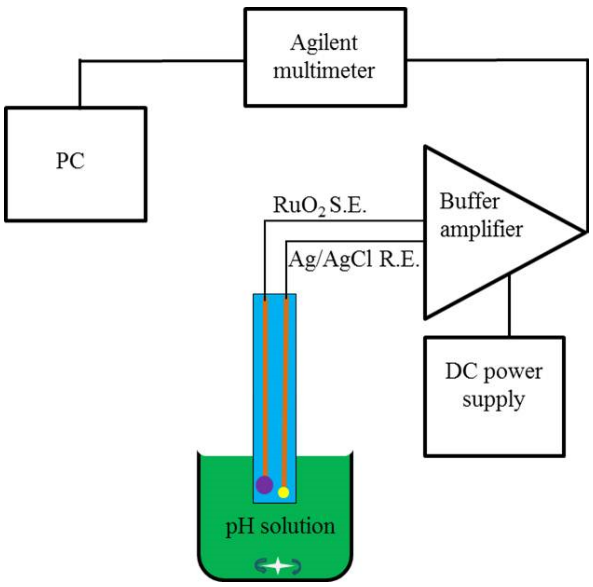

Figure 3. Measured sensor potential *versus* pH value for different RuO_2 thin-film thicknesses. Reprint with permission from [21]. Copyright 2014 Elsevier.

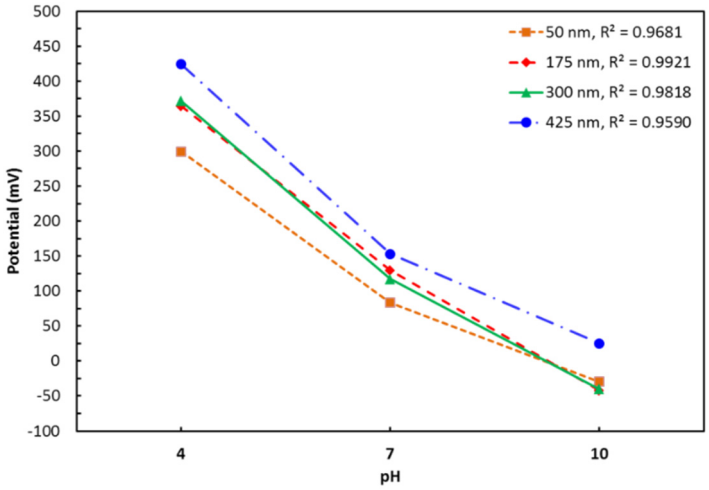

Figure 4. Measured response time *versus* sensing film thickness for test solutions of different pH values. Reprint with permission from [21]. Copyright 2014 Elsevier.

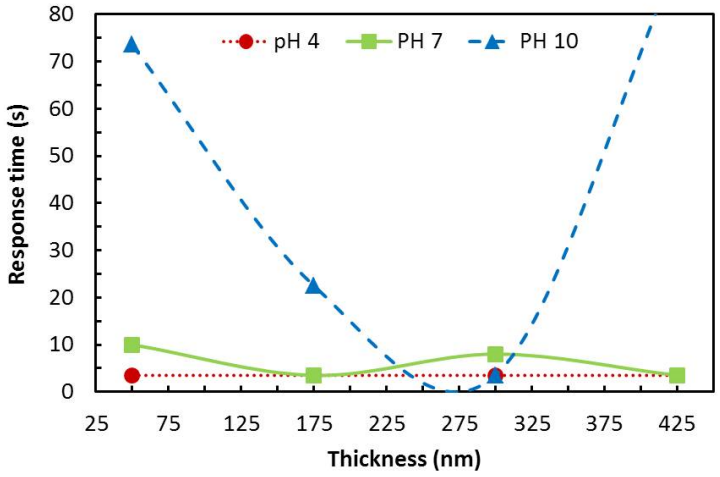

Figure 5. Measured potential in pH 4-7-10 to demonstrate stability. Reprint with permission from [21]. Copyright 2014 Elsevier.

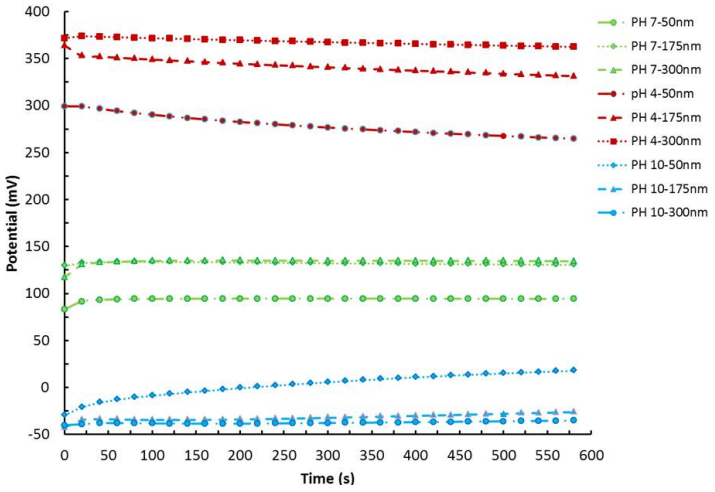

Figure 6. Measured average potential *versus* time in pH loop (4-7-10-7-4) for different RuO_2 film thickness. Reprint with permission from [21]. Copyright 2014 Elsevier.

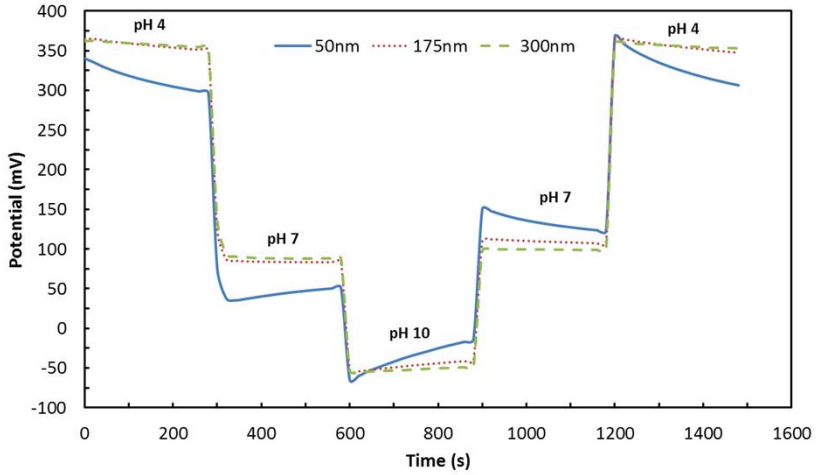

Various materials deposited using magnetron sputtering are listed in Table 1. These materials have been widely studied for pH sensing application including water quality, engine oil oxidation detection, Coca-Cola, base water, lemon, wine, vinegar, milk, seawater and hard clam (*meretrix lusoria*) cultivated solutions, glucose concentration, total cholesterol concentration and biosensor applications.

Y. H. Liao *et al.* [22] have used RuO_2 thin film as the sensing layer of hydrogen ion selective electrodes (ISE) for pH array sensors. The RuO_2 pH-sensing membrane was prepared using the R.F. sputtering system at a process pressure of 10 mTorr in $Ar:O_2$ = 4:1 gas ratio at an R.F. power of 100 W for 1 h. The pH sensitivity of the RuO_2 sensing membrane for the developed ISE devices was about 55.64 mV/pH and the drift rate was 0.38 mV/h for a pH 7 buffer solution. The hysteresis widths of the RuO_2 ISE device were 4.36 mV and 2.2 mV in pH 7-4-7-10-7 and pH 7-10-7-4-7 loop cycles, respectively. J. Chou *et al.* [23] have investigated reactively sputtered ruthenium oxide (RuO_x) and ruthenium nitride (RuN) sensing membrane deposited on silicon substrate for pH sensing applications. The RuO_x film was prepared in an Ar/O_2 process gas ratio of 40 sccm/15 sccm at an R.F. power of 100 W with a 10 mTorr pressure for 60 min. A linear pH sensitivity of 55.52 mV/pH was reported for pH values between 1 and 12 at room temperature. Moreover, in order to increase the sensing range of the pH sensor, the RuN was deposited in an Ar/O_2 process gas ratio of 15 sccm/30 sccm at 10 mTorr for 1 h with an R.F. power of 100 W. The RuN membrane exhibited a linear pH sensitivity of 57.05 mV/pH over a pH range of 1–13 at room temperature. Additionally, RuO_x/Si sensing membrane tested for the detection of the penicillin G showed a rapid response time of 35 s in comparison to 120 s response time of SnO_2/ITO. M. Chen *et al.* [28] have developed a Ta_2O_5 based capacitive electrolyte-ion sensitive membrane-oxide-semiconductor (EIOS) pH sensor and investigated its performance by means of electrochemical impedance spectroscopy (EIS) and capacitance-voltage (C-V) measurements. A 60 nm Ta film was R.F. sputtered onto oxidized silicon substrate in an Ar atmosphere at 3.3 mTorr working pressure with an R.F. power of 300 W for 5 min. Subsequently, the Ta_2O_5 film was obtained by the oxidation of the Ta layer in oxygen atmosphere for about 3 h at 525 °C, which resulted in a Ta_2O_5 film thickness of about 155 nm. Electrochemistry measurements were carried out on an advanced two-electrode electrochemical system, with a conventional Ag/AgCl (3 M KCl) electrode being the reference electrode. A Nernstian

response of ~56.19 mV/pH in the pH range 1 to 10 was attained. The EIS measurement revealed that the space charge capacitance can easily distinguish pH changes.

C. Tsai *et al.* [68] have studied the pH sensing characteristics and hysteresis effect of the R.F. sputtered tin oxide (SnO_2) electrode. The hysteresis experiments were carried out with short pH loop (7-4-7-10-7) and long pH loop (7-2-7-12-6). The hysteresis value was less than 7 mV in short pH loop and 9 mV for pH 7 in acid side (H_A) and 11 mV in alkali side (H_B). The reported pH sensitivity of the SnO_2 was about 59 mV/pH for pH range of 2–12. J. C. Chou *et al.* [69] have carried out long-term monitoring of sea water using solid-state TiO_2:Ru sensing electrodes for hard clam cultivation. In this study, a co-sputtering system was used to fabricate the TiO_2:Ru sensing film deposited on a p-type silicon substrate. The co-sputtering parameters were: R.F. power of 100 W, D.C. power of 30 W, process pressure 30 mTorr and Ar/O_2 ratio of 40 sccm/2 sccm, and a sputtering time of 60 min. The mean sensitivity and linearity of the TiO_2:Ru sensing electrode were 55.20 mV/pH and 0.999, respectively, over a pH range of 1–13. Particularly, the TiO_2:Ru sensing electrode was able to measure the pH levels for two sample solutions of pH 8 and 9, confirming the weak alkali range and suitable *meretrix lusoria* growth. L. M. Kuo *et al.* [70] have reported a precise pH microsensor developed using R.F. sputtering of iridium oxide (IrO_2) and tantalum pentoxide (Ta_2O_5) films on Pt-electrode. In their study, an easily implemented surface modification scheme was adopted, based on employing a Ta_2O_5 membrane that covers the IrO_2 electrode, making the sensor insensitive to H^+ ions and hence eliminating redox species interference. The sensitivity of the sensor was in the range of 59.44–59.50 mV/pH for the pH range 2–13. Furthermore, the pH sensor displayed high ion selectivity with respect to K^+, Na^+, and Li^+ with log $K_{H,M}$ values (~−12.4) with a working lifetime exceeding one week.

W. Bunjongpru *et al.* [71] have developed pH-ISFET sensor using CMOS compatible processes. A nanocrystalline-aluminum nitride (AlN) thin film (acted as an ion-sensitive membrane) was prepared by reactive gas-timing R.F. magnetron sputtering without heating the substrate and post annealing. In a conventional reactive gas-timing sputtering system, the feeding gas is on-off controlled periodically in such a way that the deposited AlO_xN_y film has a quite stable composition of aluminum, nitrogen and oxygen (Al:O:N = 52:18:30%) all over the entire film area. The deposition parameters used for the preparation of AlN films of various thicknesses (20, 40, 80 nm) were 12 sccm Ar and 7 sccm N_2 gas flow, gas-timing ($Ar:N_2$ = 10 s:90 s), and an R.F. power of 200 W, without heating the substrate. The pH-sensitivity characteristics showed that the pH sensitivity increases with increasing the film thickness. The highest pH-sensitivity attained was 54.50 mV/pH, for an AlN layer thickness of 80 nm. J. Chou *et al.* [72] have investigated the current-voltage characteristics of an ion-sensitive field effect transistor (ISFET) to determine the pH value at the point of zero charge (pH_{pzc}) of a pH-ISFET device comprising a 25 nm TiO_2 sensing membrane R.F. sputtered for 120 min at a pressure of 30 mTorr in Ar/O_2 = 80 sccm/20 sccm gas mixture and an R.F. power of 150 W. A pH_{pzc} value of about 6.2 at 25 °C was reported. pH sensitivities of 51.81, 54.01, 56.21, 58.41, 60.71, 63.01 mV/pH were attained at 5, 15, 25, 35, 45 and 55 °C, respectively.

L. M. Kuo *et al.* [73] have developed a pH-sensor using an R.F. sputtered WO_3/IrO_2 diode, which was sealed thoroughly by an Al_2O_3 encapsulation layer, and investigated the diode-like current-voltage characteristics of the sensor in response to hydrogen-ions. To develop the pH-sensor structure, an RF-sputtering of the WO_3 target (99.99% pure) was carried out in Ar + 35% O_2 at a pressure of 45 mTorr and a temperature of 100 °C. Subsequently, an annealing process was carried out in a high temperature

(350 °C) chamber at a pressure of 15 mTorr for 3.5 h. The IrO_2 film was also fabricated by R.F. sputtering using an iridium target (99.95% pure) at a pressure of 60 mTorr using Ar and 50% O_2 as process gases. Next, the Al_2O_3 film was R.F. magnetron sputtered using an Al_2O_3 target (99.99% pure) at a process pressure of 70 mTorr in Ar and 50% O_2 process gases for 1.5 h. The measured thickness of the WO_3, IrO_2 and Al_2O_3 films were 300 nm, 120 nm and 25 nm, respectively. The solid-state sensor exhibited good stability, repeatability and reversibility in various pH environments ranging from pH 2 to 12 at room temperature. The pH-sensor sensitivity was 0.168 μA/pH for pH 2–12. It was concluded that the chemically sensitive device would be useful for the construction of durable microsensors for tracing the acidity in environmental and biological applications.

M. Brischwein *et al.* [74] have demonstrated R.F. sputtered ruthenium oxide sensors for extracellular recording of cell-mediated pH changes in cell culture media. In this study, ruthenium oxide was directly grown with MCF-7 and L 929 cells and found to be fully biocompatible. The measured pH sensitivity range was 52–58 mV/pH and the sensor's response was almost linear between pH 5.5–11. The drift rate of the sensor was typically in the range of 1–2 mV/h. It was also reported that an increase in the thickness of the ruthenium oxide layer increases in response time and decreases in drift rate. In addition, it was observed that the pronounced redox cross-sensitivity of ruthenium oxide is a limiting factor in situations where the concentration of dissolved oxygen is not constant or cannot be directly measured. The observed sensitivity to dissolved oxygen was ~0.2 mV/hPa. Furthermore, ruthenium oxide spots on ceramic sensor chips were used for an exemplary cell based assay with MCF-7 cells, demonstrating an extracellular acidification response to the alkaloid drug cytochalasin B. In comparison with optochemical pH-sensors used for the quantification of extracellular acidification, metal oxides may be directly grown with cells and the active area of sensor spots can be made considerably small. They do not suffer from a gradual decline of performance during operation and they are not affected by interfering fluorescent substances.

J. Her *et al.* [75] have developed a highly pH sensitive electrolyte-insulator-semiconductor (EIS) device incorporating Gd_2O_3 and $GdTi_xO_y$ sensing films deposited on silicon substrates through reactive R.F. sputtering for biomedical engineering applications. A 40 nm Gd_2O_3 film was deposited on a silicon substrate by reactive R.F. sputtering from a gadolinium oxide target in diluted O_2 environment (Ar/O_2 = 5 sccm/2 sccm) at a substrate temperature of 27 °C, whereas a 40 nm $GdTi_xO_y$ film was deposited by reactive R.F. co-sputtering from both gadolinium and titanium targets in the same diluted O_2 environment. All samples were annealed in a rapid thermal annealing oven in an O_2 environment at selected reaction temperatures in the range of 700–900 °C for 30 s. Compared with Gd_2O_3 sensing membranes, the EIS device featuring $GdTi_xO_y$ sensing membrane annealed at 900 °C exhibited the highest sensitivity of 64.13 mV/pH for pH 2–12, a smaller hysteresis voltage of 1 mV for the pH loop 7-4-7-10-7 and a lower drift rate of 0.4 mV/h in a pH 7 buffer solution. The high pH sensitivity was attributed to the high surface roughness of the sensing film. Finally, the detection of glucose in serum was successfully demonstrated using EIS with glucose oxidase-immobilized alginate films. The concentration of serum glucose measured by the $GdTi_xO_y$ EIS biosensor was comparable to that determined by a commercial assay kit. The $GdTi_xO_y$ glucose biosensor can detect glucose with reasonable sensitivity (8.37 mV/mM) in solutions containing glucose of concentrations in the range 0.5–6 mM, making them suitable for general blood glucose monitoring.

6. Conclusions

Recent developments of magnetron sputtered thin films for pH sensing applications have been reviewed in this paper. Various metal oxide pH-sensing structures prepared by R.F. magnetron sputtering have been used for pH sensing applications. We have discussed the potential of various metal oxide based pH sensing electrodes, and highlighted the unique properties of ruthenium oxide and iridium oxide electrodes for pH-sensing applications, such as high sensitivity, good potential stability, wide temperature range, fast response and outstanding corrosion resistance. Furthermore, various applications of magnetron sputtered pH sensors have been discussed, including fluid quality analysis, glucose and cholesterol concentration monitoring and biosensing.

Acknowledgments

This research was supported by Edith Cowan University, Australia, and the Department of Industry, Innovation, Science, Research and Tertiary Education, Australian Government.

Author Contributions

D. K. Maurya drafted and organised this review article. A. Sardarinejad focused on the information about the pH sensing materials and references. K. Alameh reviewed the manuscript. All authors have read and approved the final manuscript.

Conflicts of Interest

The authors declare no conflict of interest.

References

1. Fierro, S.; Seishima, R.; Osamu, N.; Hideyuki, S.; Yasuaki, E. *In vivo* pH monitoring using boron doped diamond microelectrode and silver needles: Application to stomach disorder diagnosis. *Sci. Rep.* **2013**, *3*, doi:10.1038/srep03257.
2. Kohlmann, F.J. *What is pH, and How is it Measured*? *A Technical Handbook for Industry*; Hach Company: Loveland, CO, SUA, 2003.
3. Korostynska, O.; Arshak, K.; Gill, E.; Arshak, A. Review on state-of-the-art in polymer based pH sensors. *Sensors* **2007**, *7*, 3027–3042.
4. Privett, B.J.; Shin, J.H.; Schoenfisch, M.H. Electrochemical sensors. *Anal. Chem.* **2010**, *82*, 4723–4741.
5. Huang, W.D.; Cao, H.; Deb, S.; Chiao, M.; Chiao, J.C. A flexible pH sensor based on the iridium oxide sensing film. *Sens. Actuators A Phys.* **2011**,*169*, 1–11.
6. Eftekhari, A. pH sensor based on deposited film of lead oxide on aluminum substrate electrode. *Sens. Actuators B Chem.* **2003**, *3*, 234–238.
7. Van der Schoot, B.H.; Bergveld, P. ISFET based enzyme sensors. *Biosensors* **1987**, *3*, 161–186.
8. Yuqing, M.; Jianguo, G.; Jianrong, C. Ion sensitive field effect transducer-based biosensors. *Biotechnol. Adv.* **2003**, *21*, 527–534.

9. Lee, C.; Kim, S.K.; Kim, M. Ion-sensitive field-effect transistor for biological sensing. *Sensors* **2009**, *9*, 7111–7131.
10. Olthuis, W.; Robben, M.A.M.; Bergveld, P.; Bos, M.; Van der Linden, W.E. pH sensor properties of electrochemically grown iridium oxide. *Sens. Actuators B Chem.* **1990**, *2*, 247–256.
11. Kinlen, P.J.; Heider, J.E.; Hubbard, D.E. A solid-state pH sensor based on a nafion-coated iridium oxide indicator electrode and a polymer-based silver chloride reference electrode. *Sens. Actuators B Chem.* **1994**, *1*, 13–25.
12. Richter, A.; Paschew, G.; Klatt, S.; Lienig, J.; Arndt, K.; Adler, H.P. Review on hydrogel-based pH sensors and microsensors. *Sensors* **2008**, *1*, 561–581.
13. Gerlach, G.; Guenther, M.; Sorber, J.; Suchaneck, G.; Arndt, K.F.; Richter, A. Chemical and pH sensors based on the swelling behavior of hydrogels. *Sens. Actuators B Chem.* **2005**, *111–112*, 555–561.
14. Bezbaruah, A.N.; Zhang, T.C. Fabrication of anodically electrodeposited iridium oxide film pH microelectrodes for microenvironmental studies. *Anal. Chem.* **2002**, *74*, 5726–5733.
15. Ges, I.A.; Ivanov, B.L.; Schaffer, D.K.; Lima, E.A.; Werdich, A.A.; Baudenbacher, F.J. Thin-film IrO_x pH microelectrode for microfluidic-based microsystems. *Biosens. Bioelectron.* **2005**, *2*, 248–256.
16. Kim, T.Y.; Yang, S. Fabrication method and characterization of electrodeposited and heat-treated iridium oxide films for pH sensing. *Sens. Actuators B Chem.* **2014**, *196*, 31–38.
17. Nguyen, C.M.; Huang, W.; Rao, S.; Cao, H.; Tata, U.; Chiao, Mu.; Chiao, J. Sol-Gel iridium oxide-based pH sensor array on flexible polyimide substrate. *IEEE Sens. J.* **2013**, *10*, 3857–3864.
18. Nguyen, C.M.; Rao, S.; Seo, Y.; Schadt, K.; Hao, Y.; Chiao, J.C. Micro pH sensors based on iridium oxide nanotubes. *IEEE Trans. Nanotechnol.* **2014**, *5*, 945–953.
19. Prats-Alfonso, E.; Abad, L.; Casañ-Pastor, N.; Gonzalo-Ruiz, J.; Baldrich, E. Iridium oxide pH sensor for biomedical applications. Case urea–urease in real urine samples. *Biosens. Bioelectron.* **2013**, *1*, 163–169.
20. Maurya, D.K.; Sardarinejad, A.; Alameh, K. High-sensitivity pH sensor employing a sub-micron ruthenium oxide thin-film in conjunction with a thick reference electrode. *Sens. Actuators A Phys.* **2013**, *203*, 300–303.
21. Sardarinejad, A.; Maurya, D.K.; Alameh, K. The effects of sensing electrode thickness on ruthenium oxide thin-film pH sensor. *Sens. Actuators A Phys.* **2014**, *214*, 15–19.
22. Liao, Y.-H.; Chou, J.-C. Preparation and characteristics of ruthenium dioxide for pH array sensors with real-time measurement system. *Sens. Actuators B Chem.* **2008**, *128*, 603–612.
23. Chou, J.; Liu, S.; Chen, S. Sensing characteristics of ruthenium films fabricated by radio frequency sputtering. *Jpn. J. Appl. Phys.* **2005**, *3*, 1403–1408.
24. Zhuiykov, S.; O'Brien, D.; Best, M. Water quality assessment by an integrated multi-sensor based on semiconductor RuO_2 nanostructures. *Meas. Sci. Technol*. **2009**, *20*, doi:10.1088/0957-0233/20/9/095201.
25. Fog, A.; Buck, R.P. Electronic semiconducting oxides as pH sensors. *Sens. Actuators* **1984**, *5*, 137–146.
26. Chou, J.C.; Liu, C.H.; Chen, C.C. Electrochromic property of sol-gel derived TiO_2 thin film for pH sensor. *IFMBE Proc*. **2011**, *35*, 69–72.

27. Bahari, N.; Zain, A.M.; Abdullah, A.Z.; Sheng, D.B.C.; Othman, M. Study on pH sensing properties of RF magnetron sputtered tantalum pentoxide (Ta_2O_5) thin film. In Proceedings of 2010 IEEE International Conference on Semiconductor Electronics, Melaka, Malaysia, 28–30 June 2010; pp. 76–78.
28. Chen, M.; Jin, Y.; Qu, X.; Jin, Q.; Zhao, J. Electrochemical impedance spectroscopy study of Ta_2O_5 based EIOS pH sensors in acid environment. *Sens. Actuators B Chem.* **2000**, *71*, 73–76.
29. Jeon, D.; Yoo, W.J.; Seo, J.K.; Shin, S.H.; Han, K.; Kim, S.G.; Park, J.; Lee, B. Fiber-optic pH sensor based on Sol-Gel film immobilized with neutral red. *Opt. Rev.* **2013**, *2*, 209–213.
30. Glanc-Gostkiewicz, M.; Sophocleous, M.; Atkinson, J.K.; Garcia-Breijo, E. Performance of miniaturized thick-film solid state pH sensors. *Sens. Actuators A Phys.* **2013**, *202*, 2–7.
31. Veeramani, M.S.; Shyam, P.; Ratchagar, N.P.; Chadha, A.; Bhattacharya, E.; Pavan, S. A miniaturized pH sensor with an embedded counter electrode and a readout circuit. *IEEE Sens. J.* **2013**, *5*, 1941–1948.
32. Choi, S.; Park, I.; Hao, Z.; Holman, H.N.; Pisano, A.P. Quantitative studies of long-term stable, top-down fabricated silicon nanowire pH sensors. *Appl. Phys. A* **2012**, *107*, 421–428.
33. Huang, X.; Ren, Q.; Yuan, X.; Wen, W.; Chen, W.; Zhan, D. Iridium oxide based coaxial pH ultramicroelectrode. *Electrochem. Commun.* **2014**, *40*, 35–37.
34. Grieger, C.; Köster, F. Creation of functional layers for pH sensors by galvanic deposition of antimony and bismuth. *Sci. J. Chem*. **2014**, *2*, 6–10.
35. Lee, Y.; Park, J. Fabrication and characterization of multilayered nanoporous platinum films deposited by electroplating and nonionic surfactant molds. *Appl. Surf. Sci.* **2013**, *277*, 100–104.
36. Kelly, P.J.; Arnell, R.D. Magnetron sputtering: A review of recent developments and applications. *Vacuum* **2000**, *56*, 159–172.
37. Musil, J.; Baroch, P.; Viček, J.; Nam, K.H.; Han, J.G. Reactive magnetron sputtering of thin films: Present status and trends. *Thin Solid Films* **2005**, *1–2*, 208–218.
38. Alam, M.N.; Vasiliev, M.; Kotovb, V.; Alameh, K. Recent developments in magneto-optic garnet-type thin-film materials synthesis. *Procedia Eng.* **2014**, *76*, 61–73.
39. Alam, M.N.; Vasiliev, M.; Alameh, K. Bi3Fe5O12:Dy2O3 composite thin film materials for magneto-photonics and magneto-plasmonics. *Opt. Mater. Express* **2014**, *4*, 1866–1875.
40. Alam, M.N.; Vasiliev, M.; Alameh, K. Nano-structured magnetic photonic crystals for magneto-optic polarization controllers at the communication-band wavelengths. *Opt. Quantum Electron.* **2009**, *41*, 661–669.
41. Michael, W.W.; Aiello, Z.T.; Berliner, A.; Banerjee, P.; Zhou, S. *In-situ* immobilization of quantum dots in polysaccharide-based nanogels for integration of optical pH-sensing, tumor cell imaging, and drug delivery. *Biomaterials* **2010**, *11*, 3023–3031.
42. Zamarreño, C.R.; Hernáez, M.; Villar, I.D.; Matías, I.R.; Arregui, F.J. Optical fiber pH sensor based on lossy-mode resonances by means of thin polymeric coatings. *Sens. Actuators B Chem.* **2011**, *155*, 290–297.
43. Wu, W.; Mitra, N.; Yan, E.C.Y.; Zhou, S. Multifunctional hybrid nanogel for integration of optical glucose sensing and self-regulated insulin release at physiological pH. *ACS Nano* **2010**, *8*, 4831–4839.

44. Li, J.; Huang, X.; Xu, W.; Xiao, D.; Zhong, Z. A fiber-optic pH sensor based on relative Fresnel reflection technique and biocompatible coating. *Opt. Fiber Technol.* **2014**, 28–31.
45. Shao, L.; Yin, M.; Tam, H.; Albert, J. Fiber optic pH sensor with self-assembled polymer multilayer nanocoatings. *Sensors* **2013**, *2*, 1425–1434.
46. Bakker, E.; Qin, Y. Electrochemical sensors. *Anal. Chem.* **2006**, *78*, 3965–3983.
47. Rahman, M.A.; Kumar, P.; Park, D.; Shim, Y. Electrochemical sensors based on organic conjugated polymers. *Sensors* **2008**, *1*, 118–141.
48. Wang, F.; Hu, S. Electrochemical sensors based on metal and semiconductor nanoparticles. *Microchim. Acta* **2009**, *1–2*, 1–22.
49. Kimmel, D.W.; LeBlanc, G.; Meschievitz, M.E.; Cliffel, D.E. Electrochemical sensors and biosensors. *Anal. Chem.* **2012**, *84*, 685–707.
50. Nie, Z.; Nijhuis, C.A.; Gong, J.; Chen, X.; Kumachev, A.; Martinez, A.W.; Narovlyansky, M.; Whitesides, G.M. Electrochemical sensing in paper-based microfluidic devices. *Lab Chip* **2010**, *10*, 477–483.
51. Lakard, B.; Segut, O.; Lakard, S.; Herlem, G.; Gharbi, T. Potentiometric miniaturized pH sensors based on polypyrrole films. *Sens. Actuators B Chem.* **2007**, *1*, 101–108.
52. Bandodkar, A.J.; Hung, V.W.S.; Jia, W.; Valdés-Ramírez, G.; Windmiller, J.R.; Martinez, A.G.; Ramírez, J.; Chan, G.; Kerman, K.; Wang, J. Tattoo-based potentiometric ion-selective sensors for epidermal pH monitoring. *Analyst* **2013**, *138*, 123–128.
53. Guinovart, T.; Valdés-Ramírez, G.; Windmiller, J.R.; Andrade, F.J.; Wang, J. Bandage-based wearable potentiometric sensor for monitoring wound pH. *Electroanalysis* **2014**, *6*, 1345–1353.
54. Zuliani, C.; Matzeu, G.; Diamond, D. A potentiometric disposable sensor strip for measuring pH in saliva. *Electrochim. Acta* **2014**, *132*, 292–296.
55. Li, Q.; Li, H.; Zhang, J.; Xu, Z. A novel pH potentiometric sensor based on electrochemically synthesized polybisphenol a films at an ITO electrode. *Sens. Actuators B Chem.* **2011**, *2*, 730–736.
56. Das, At.; Das, An.; Chang, L.B.; Lai, C.; Lin, R.M.; Chu, F.C.; Lin, Y.H.; Chow, L.; Jeng, M.J. GaN thin film based light addressable potentiometric sensor for pH sensing application. *Appl. Phys. Express* **2013**, *6*, doi:10.7567/APEX.6.036601.
57. Lee, H.C.; Zhang, L.F.; Lu, C.H.; Lin, J.L.; Chin, Y.L.; Sun, T.P. Development of anodic titanium oxide nanotubes applied to a pH sensor with amperometric and potentioimetric methods. *Adv. Mater. Res.* **2012**, *528*, 10–13.
58. Shim, J.H.; Kang, M.; Lee, Y.; Lee, C. A nanoporous ruthenium oxide framework for amperometric sensing of glucose and potentiometric sensing of pH. *Microchim. Acta* **2012**, *177*, 211–219.
59. Stred'anský, M.; Pizzariello, A.; Stred'anská, S.; Miertuš, S. Amperometric pH-sensing biosensors for urea, penicillin, and oxaloacetate. *Anal. Chim. Acta* **2000**, *1–2*, 151–157.
60. Pizzariello, A.; Stredanský, M.; Stredanská, S.; Miertuš, S. Urea biosensor based on amperometric pH-sensing with hematein as a pH-sensitive redox mediator. *Talanta* **2001**, *4*, 763–772.
61. Gao, W.; Song, J. Polyaniline film based amperometric pH sensor using a novel electrochemical measurement system. *Electroanalysis* **2009**, *8*, 973–978.
62. Schwarz, M.A.; Hauser, P.C. Recent developments in detection methods for microfabricated analytical devices. *Lab Chip* **2001**, *1*, 1–6.

63. Xu, J.; Bao, N.; Xia, X.; Peng, Y.; Chen, H. Electrochemical detection method for nonelectroactive and electroactive analytes in microchip electrophoresis. *Anal. Chem.* **2004**, *23*, 6902–6907.
64. Zhang, X. Nitric oxide (NO) electrochemical sensors. In *Electrochemical Sensors, Biosensors and Their Biomedical Applications*; Zhang, X., Ju, H., Wang, J., Eds.; Academic Press: Waltham, MA, USA, 2011.
65. Liao, Y.; Chou, J. Fabrication and characterization of a ruthenium nitride membrane for electrochemical pH sensors. *Sensors* **2009**, *9*, 2478–2490.
66. Chin, Y.L.; Chou, J.C.; Lei, Z.C.; Sun, T.P.; Chung, W.Y.; Hsiung, S.K. Titanium nitride membrane application to extended gate field effect transistor pH sensor. *Jpn. J. Appl. Phys*. **2001**, *40*, 6311–6315.
67. Harsanyi, G. *Sensors in Biomedical Applications: Fundamentals, Technology and Applications*; CRC Press LCC: Boca Raton, FL, USA, 2000.
68. Tsai, C.; Chou, J.; Sun, T.; Hsiung, S. Study on the sensing characteristics and hysteresis effect of the tin oxide pH electrode. *Sens. Actuators B Chem.* **2005**, *108*, 877–882.
69. Chou, J.; Chen, C. Long-term monitor of seawater by using TiO_2:Ru sensing electrode for hard calm cultivation. *Eng. Technol.* **2009**, *53*, 303–307.
70. Kuo, L.; Chou, Y.; Chen, K.; Lu, C.; Chao, S. A precise pH microsensor using RF-sputtering IrO_2 and Ta_2O_5 films on Pt-electrode. *Sens. Actuators B Chem.* **2014**, *193*, 687–691.
71. Bunjongpru, W.; Porntheeraphat, S.; Trithaveesak, O.; Somwang, N.; Khomdet, P.; Jeamsaksiri, W.; Hruanun, C.; Poyai, A.; Nukeaw, J. The innovative AlN-ISFET based pH sensor. In Proceeds of ECTI-CON 2008. 5th International Conference on Electrical Engineering/Electronics, Computer, Telecommunications and Information Technology, Krabi, Thailand, 14–17 May 2008; pp. 833–836.
72. Chou, J.; Laio, L. Study on pH at the point of zero charge of TiO_2 pH ion-sensitive field effect transistor made by the sputtering method. *Thin Solid Films* **2005**, *476*, 157–161.
73. Kuo, L.; Chen, K.; Chuang, Y.; Chao, S. A flexible pH-sensing structure using WO_3/IrO_2 junction with Al_2O_3 encapsulation layer. *ECS Solid State Lett.* **2013**, *3*, 28–30.
74. Brischwein, M.; Grothe, H.; Weist, J.; Zottmann, M.; Ressler, J.; Wolf, B. Planar ruthenium oxide sensors for cell-on-a-chip metabolic studies. *Chem. Anal. (Warsaw)* **2009**, *54*, 1193–1201.
75. Her, J.; Wu, M.; Peng, Y.; Pan, T.; Weng, W.; Pang, S.; Chi, L. High performance $GdTi_xO_y$ electrolyte-insulator-semiconductor pH Sensor and biosensor. *Int. J. Electrochem. Sci.* **2013**, *8*, 606–620.